

Interplay of antiferromagnetism, ferromagnetism and superconductivity in $\text{EuFe}_2(\text{As}_{1-x}\text{P}_x)_2$ single crystals

H. S. Jeevan,¹ Deepa Kasinathan,² Helge Rosner,² and Philipp Gegenwart¹

¹*I. Physikalisches Institut, Georg-August-Universität Göttingen, D-37077 Göttingen, Germany and*

²*Max-Planck-Institut für Chemische Physik fester Stoffe, 01187 Dresden, Germany*

We report a systematic study on the influence of antiferromagnetic and ferromagnetic phases of Eu^{2+} moments on the superconducting phase upon doping the As site by isovalent P, which essentially acts like chemical pressure on EuFe_2As_2 . Bulk superconductivity with transition temperatures of 22 K and 28 K are observed for $x=0.16$ and 0.20 samples, respectively. The Eu ions order antiferromagnetically for $x \leq 0.13$, while a crossover is observed for $x \geq 0.22$ whereupon the Eu ions order ferromagnetically. Density functional theory based calculations reproduce the observed experimental findings consistently. We discuss in detail the coexistence of superconductivity and magnetism in a tiny region of the phase space and comment on the competition of ferromagnetism and superconductivity in the title compound.

PACS numbers: 71.20.Eh, 75.10.Dg, 75.20.Hr

The appearance of superconductivity (SC) in the vicinity of a magnetic instability is often related to quantum critical phenomena,^{1,2} although only in few cases the magnetic excitations which mediate the SC pairing have been identified.³ The discovery of superconductivity upon suppression of magnetism in iron containing pnictides and chalcogenides has created great interest in the field of condensed matter physics. Among the various members of the iron containing pnictides, there are three main family of materials, which show SC transitions upon substitution by a dopant or upon applying external pressure. They are, (i) the quaternary ‘1111’ compounds, $R\text{FeAsO}$, where R represents a lanthanide such as La, Ce, Sm etc.^{4–7} with transition temperatures as high as 56 K; (ii) the ternary $A\text{Fe}_2\text{As}_2$ ($A = \text{Ca}, \text{Sr}, \text{Ba}, \text{Eu}$)^{8–11} systems, also known as ‘122’ systems that exhibit superconductivity up to 38 K; and (iii) the binary chalcogenide ‘11’ systems (*eg.* FeSe) with superconducting transition temperatures upto 14 K.¹² In general, the magnetism occurring in the Fe sublattice can be suppressed by doping via two schemes: (i) direct doping of Fe in the FeAs layer by Co, Ni, Rh, (electron doping)^{13,14} or Ru (isovalent substitution)¹⁵ (ii) indirect doping on other sites which includes, oxygen by fluorine in the ‘1111’ systems (electron doping),⁴ alkaline earth metals by alkaline metals in the ‘122’ systems (hole doping),⁸ and arsenic with phosphorus (isovalent substitution).^{16,17} Similar to doping, external pressure also facilitates the suppression of Fe magnetism.¹⁸ In the case of rare-earth based iron pnictides, a second magnetic sublattice, due to the localized f -moments comes into play additionally to the Fe sublattice. In general, the rare-earth ions tend to order antiferromagnetically, thereby introducing only a weak coupling between the two sublattices. In this work we concentrate on EuFe_2As_2 , the only rare-earth based member of the ‘122’ family. EuFe_2As_2 exhibits a spin density wave (SDW) in the Fe sublattice together with a structural transition at 190 K and in addition an A-type antiferromagnetic (AF) order at 19 K due to Eu^{2+} ions (ferromagnetic layers ordered antiferromagnetically).¹⁹ Supercon-

ductivity can be achieved in this system by substituting Eu with K or Na (Ref. 9 and 20), As with P (Ref. 21) and upon application of external pressure.^{18,22} Pressure studies upto 3 GPa on the parent compound have also shown indications of *reentrant* SC, akin to ternary Chevrel phases or rare-earth nickel borocarbides.¹⁸

Isovalent P doping on the As site in EuFe_2As_2 without introducing holes or electrons, simulates a scenario generally referred to as “chemical pressure”. While the Eu^{2+} moments order antiferromagnetically (A-type) at 19 K in the parent compound, ferromagnetic order at 27 K is found for the end member EuFe_2P_2 .²³ In early 2009, Ren and coworkers²¹ reported on the co-existence of SC and ferromagnetism (FM) of the Eu^{2+} moments in polycrystalline samples of $\text{EuFe}_2(\text{As}_{0.7}\text{P}_{0.3})_2$, with a superconducting transition at 26 K, followed by a FM ordering of the Eu^{2+} moments at 20 K. Recently, another report²⁴ also documents the co-existence of SC (at 26 K) and FM (at 18 K) in $\text{EuFe}_2(\text{As}_{0.73}\text{P}_{0.27})_2$ along with a reentrant behavior below 16 K. On the other hand systematic studies by Ren and collaborators on Ni doping in $\text{EuFe}_{2-x}\text{Ni}_x\text{As}_2$ showed only FM ordering of the Eu^{2+} moments but no superconductivity.²⁵ In contrast, superconductivity has been reported upon Ni doping of the Fe site for the other three members of the $A\text{Fe}_{2-x}\text{Ni}_x\text{As}_2$ ($A = \text{Ca}, \text{Sr}, \text{Ba}$) family.^{14,26–28} Based on these reports, the physical properties of both Ni and P doped EuFe_2As_2 samples seem to contradict each other in terms of competition or coexistence of FM and SC phases. In this paper, we report on the detailed investigation of the resistivity, magnetization and specific heat measurements using well-characterized single crystals of $\text{EuFe}_2(\text{As}_{1-x}\text{P}_x)_2$ and show the presence of bulk superconductivity up to 28 K. Our measurements also prove that in this system, the FM (Eu^{2+} ions) and SC phases compete with each other, rather than coexist, in contradiction to the claim of Ref. 21 and 24. Bulk SC coexisting with AF Eu^{2+} ordering is only found in a very narrow regime of P doping, where the Fe SDW transition has just been suppressed. The systematic study of P doping on single crystals al-

TABLE I. Tetragonal lattice parameters (for selected samples at 300 K) of $\text{EuFe}_2(\text{As}_{1-x}\text{P}_x)_2$ crystallizing in the ThCr_2Si_2 -type structure as a function of phosphorus substitution (x), which is determined by EDX

| x | a (Å) | c (Å) |
|------|---------|---------|
| 0 | 3.907 | 12.114 |
| 0.15 | 3.891 | 11.948 |
| 0.16 | 3.890 | 11.930 |
| 0.20 | 3.887 | 11.890 |
| 0.22 | 3.889 | 11.877 |
| 0.26 | 3.889 | 11.870 |
| 0.38 | 3.885 | 11.774 |
| 1 | 3.816 | 11.248 |

allows us to draw a phase diagram that is complex and rich with five different phases.

A series of single crystals of $\text{EuFe}_2(\text{As}_{1-x}\text{P}_x)_2$ with a range of P doping were synthesized using the Bridgman method. Stoichiometric amounts of starting elements (Eu 99.99%, Fe 99.99 %, As 99.99999% and P 99.99 %) were taken in an Al_2O_3 crucible, which was then sealed in a Ta-crucible under Argon atmosphere. The sealed crucible was heated at a rate of $50^\circ\text{C}/\text{hour}$ up to 1300°C , kept for 12 hours at the same temperature and then cooled to 950°C with a cooling rate of $3^\circ\text{C}/\text{hour}$. We obtained large plate-like single crystals using this process with dimensions of $5 \times 3 \text{ mm}^2$ in the ab -plane. In addition to the plate-like single crystals, we also found a secondary polycrystalline phase which was identified as Fe_2P . All the elements and sample handling were carried out inside a glove box filled with Ar atmosphere. The quality of the single crystals was checked using the Laue method, powder x-ray diffraction and additionally with scanning electron microscopy equipped with energy dispersive x-ray analysis (EDX). Electrical resistivity and specific heat were measured using a Physical Properties Measurement System (PPMS, Quantum Design, USA). Magnetic properties were measured using Superconducting Quantum Interference Device (SQUID) magnetometer procured from Quantum Design. The change of the electronic properties with phosphorus doping has been investigated by angle-resolved photoemission spectroscopy (ARPES) and optical conductivity measurements^{29–31} on our single crystals. ARPES measurements indicate that the electronic structure of the phosphorus doped systems are more 3D compared to the parent compound and as well as to the case of electron doping.^{29,30} Recent infrared spectroscopy measurements claim evidence for a single nodeless s-wave superconducting gap for isovalent substitution in contrast to the multi-gap scenario in carrier doped systems.³¹ In this paper we focus on the interplay of Eu^{2+} magnetism on the formation of SC.

The powder diffraction pattern of all the samples can be indexed using the tetragonal ThCr_2Si_2 structure type. The variation of the lattice parameters with re-

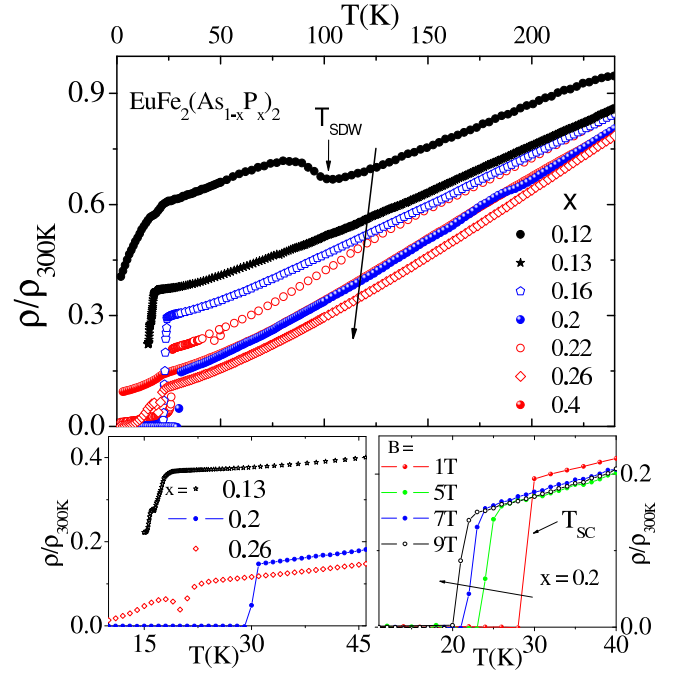


FIG. 1. (Color online) Temperature dependence of the in-plane (ab -plane) resistivity for various $\text{EuFe}_2(\text{As}_{1-x}\text{P}_x)_2$ single crystals. The data are normalized to the room temperature resistivity. Due to technical reasons, the resistivity for $x=0.13$ sample was measured down to 15 K only. The lack of SC (zero resistivity) transition is confirmed by the magnetic susceptibility measurements (Fig. 2). Lower left panel: Low temperature part of the normalized in-plane resistivity for selected samples. Lower right panel: Normalized in-plane resistivity of the superconducting sample ($x=0.2$) for various values of applied magnetic field.

spect to P content is collected in Table I, wherein the actual P content is given as determined by EDX. Similar to other isovalent substitutions of 122 systems discussed in literature³², phosphorus substitution on the As site leads to a dramatic decrease of FeAs-layer thickness, which indicates that P doping mainly affects the c lattice parameter. We also observe that the decrease along the tetragonal axis (c lattice parameter) is more pronounced compared to the changes in the ab plane (*cf.* Table I).

The temperature dependence of the normalized resistivity (with the current measured in the basal ab -plane) is shown in Fig. 1 for the single crystals of $\text{EuFe}_2(\text{As}_{1-x}\text{P}_x)_2$. The temperature dependence of the resistivity shows a metallic behavior for the entire doping range. For the parent compound EuFe_2As_2 , we observe both the SDW anomaly associated with the structural and magnetic transition of the Fe sublattice¹⁹ at 190 K (T_{SDW}) and the anomaly at 19 K (T_N) associated with the AF ordering of the Eu^{2+} moments. Upon doping with P, for the lowest P content studied here $x=0.12$, the resistivity decreases linearly with temperature down to 90 K, whereupon we observe an anomaly which is likely due to the SDW transition. We observe another anomaly around 20 K which is likely associated with the A-type

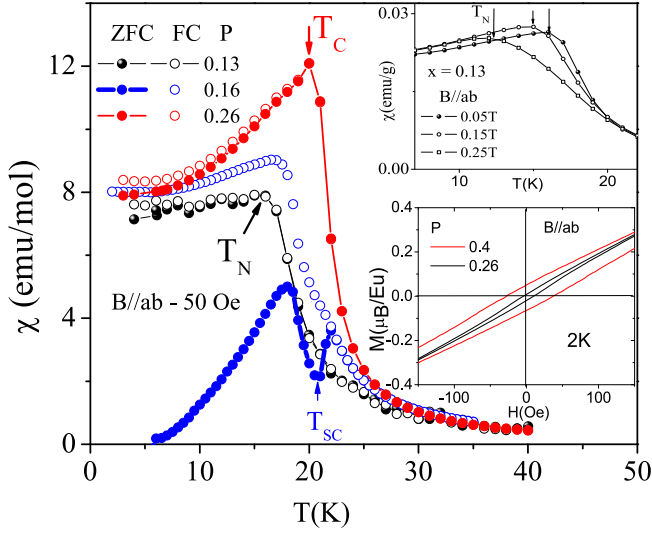


FIG. 2. (Color online) Temperature dependence of the magnetic susceptibility for $\text{EuFe}_2(\text{As}_{1-x}\text{P}_x)_2$. Upper inset: Field dependence of the AF transition for the $x=0.13$ sample. Lower inset: Isothermal magnetization at 2 K of $x=0.26$ and 0.4 samples which show a FM ordering of the Eu^{2+} moments.

AF ordering of the Eu^{2+} ions. No further anomalies are observed for this sample. When the P content is increased, the SDW transition is fully suppressed and a sudden drop in the resistivity indicative of a superconducting (SC) transition is observed for $x=0.16$ at 22 K and for $x=0.2$ at 29 K. For $x=0.22$, a sharp drop in the resistivity is observed around 25 K but the normalized resistivity does not go to zero. For larger P concentrations, $x \geq 0.26$, the SC transition is fully suppressed. Our observations described here are in contradiction to previous reports^{21,24} which evidence a SC transition around 26 K for polycrystalline samples with $x=0.27$ and 0.30. We do not observe zero resistance consistently for all samples with $x \geq 0.22$. The lower right panel of Fig. 1 shows the field dependence of the normalized resistivity of the SC transition temperature for the $x=0.2$ sample. The $\rho(T)/\rho_{300\text{K}}$ shows a sharp drop below 30 K in zero magnetic field and shifts to lower temperatures as the field increases and reaches 22 K at 9 T, in accordance with the SC properties.

We measured the dc magnetic susceptibility for selected compositions to obtain more insights regarding the nature of the magnetic and SC phases, with the applied magnetic field parallel to the ab plane. Fig. 2 shows the field cooled (FC) and zero field cooled (ZFC) susceptibility at 50 Oe, for $x = 0.13, 0.16$ and 0.26. For the under-doped sample ($x=0.13$) both ZFC and FC data show only the anomaly at 17 K due to AF ordering of the Eu^{2+} moments. There are no signs for a SC phase for this sample. For the optimally doped $x=0.16$ sample, the susceptibility shows a pronounced diamagnetic step at 22 K, evidence for a bulk SC transition, consistent with the sharp drop observed in resistivity below 22 K. Above

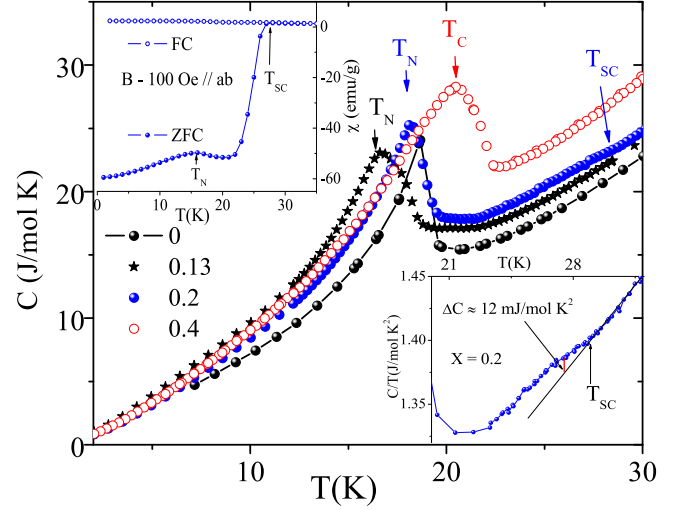


FIG. 3. (Color online) Evaluation of AF (T_N) and FM (T_C) ordering temperatures as a function of phosphorus substitution in the specific heat. Lower inset shows the anomaly of the SC phase transition for the $x=0.2$ sample. Upper inset shows the dc-magnetic susceptibility for ZFC and FC experiments in applied field of 50 Oe for the $x=0.2$ sample.

20 K the susceptibility begins to increase and reaches a maximum around 18 K, which is indicative of the AF ordering of the Eu^{2+} moments. This observation of the coexistence of SC and AF ordering for $x=0.16$ is similar to the ac-susceptibility measurements reported previously for the parent compound under 25.7 kbar pressure.²² Further increasing the P content to $x=0.26$, the magnetic susceptibility shows only an anomaly at 20 K due to the FM ordering of the Eu^{2+} moments (discussed later). It is clear from the magnetic susceptibility measurements, that bulk SC phase transition is observed only for the $x=0.16$ sample, while no sign for a SC phase is inferred for $x=0.13$ and 0.26 samples. The inset of Fig. 2 shows the field dependence of T_N for the under-doped sample, $x=0.13$. With increasing fields, T_N is shifted to lower values. This is indicative of the AF ordering of the Eu^{2+} moments. Upon increasing the P content to $x=0.26$, the Eu ordering changes from AF to FM. The FM ordering of the $x=0.26$ and 0.4 samples are confirmed by isothermal magnetization measurements at 2 K shown in the lower inset of Fig. 2. A small but clear hysteresis loop is observed as a function of applied field, which is consistent with similar observation in the ferromagnetically ($T_C=29\text{K}$) ordered end member EuFe_2P_2 .²³ Previous reports^{21,24} have claimed the coexistence of SC with FM for $x=0.27$ and 0.3 polycrystals, which display a tiny (10^{-2} emu/mol) diamagnetic contribution to the susceptibility together with a broadened resistive transition at 25 K and which also shows a re-entrance behavior around 16 K. The data on single crystals presented here indicate clear bulk SC only within the concentration range $0.16 \leq x \leq 0.2$. At large P doping, where Eu displays FM ordering, SC appears to be suppressed.

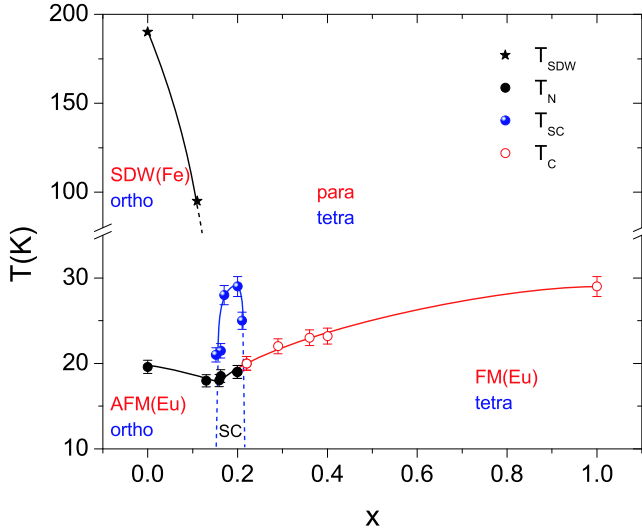


FIG. 4. (Color online) The complex phase diagram for $\text{EuFe}_2(\text{As}_{1-x}\text{P}_x)_2$ as a function of P. The solid lines act as a guide to the eye and the dotted lines are extrapolation using the available experimental data to close the superconducting dome.

Another confirmation for the bulk nature of the magnetic and SC phases is obtained by measuring the specific heat (C_p) in the temperature range from 35 K down to 2 K. The data are collected in Fig. 3 for an under-doped ($x=0.13$), optimally doped ($x=0.2$) and over-doped ($x=0.4$) single crystal. The plot shows clear anomalies for both AFM (T_N) and FM (T_C) phase transitions for $x=0.13$ and 0.4 respectively. Due to strong contributions at low temperatures from the phonons and Eu^{2+} magnetic moments to the specific heat, it is difficult to observe an anomaly at the SC phase transition, however a small anomaly (lower inset of Fig. 3) in the raw data (without subtracting any phonon contribution) is resolved below 28 K for $x=0.2$. This observation is consistent with the diamagnetic step observed in the magnetic susceptibility (upper inset of Fig. 3) as well as the drop in resistivity (Fig. 1). In addition, the magnetic susceptibility for $x=0.2$ (ZFC at 50 Oe) shows a small anomaly at 20 K corresponding to the AF transition of the Eu^{2+} moments, indicative of a co-existence of AF and SC for this sample. Based on these thermodynamic measurements, we infer that both the magnetism and SC are of bulk nature and furthermore only AF and SC phases co-exist for $\text{EuFe}_2(\text{As}_{1-x}\text{P}_x)_2$. A single crystal with $x=0.18$, displaying a SC transition at 28 K has also been studied by optical conductivity measurements³¹ above and below T_C . A BCS fit revealed a s-wave type gap with $2\Delta = 3.8k_B T_C$.

The results obtained from the different measurements allow us to draw the electronic phase diagram of $\text{EuFe}_2(\text{As}_{1-x}\text{P}_x)_2$ as a function of phosphorus doping. The transition temperatures were determined from specific heat, resistivity and magnetic susceptibility measurements. Fig. 4 shows a complex phase diagram, wherein we have identified five different phases. The

parent compound EuFe_2As_2 with tetragonal symmetry is paramagnetic at high temperatures (above 190 K), while below 190 K, the structure changes to orthorhombic and the Fe moments order antiferromagnetically (SDW). In addition, below 19 K, the system undergoes another AF transition associated with the Eu^{2+} moments. Upon isovalent doping of the As site with P in $\text{EuFe}_2(\text{As}_{1-x}\text{P}_x)_2$, for $0.16 \leq x \leq 0.22$ we observe bulk SC phase transitions coexisting with AF ordering of the Eu^{2+} moments. Further increasing the P content, $x \geq 0.26$, SC is completely suppressed and the Eu^{2+} sublattice magnetic interaction changes from AFM to FM. Recently, Nandi *et al.* proposed³³ that the coupling between orthorhombicity and superconductivity is indirect and claim that it arises due to the strong competition between magnetism (of Fe) and superconductivity in Co doped BaFe_2As_2 systems. This means that the orthorhombic to tetragonal transition occurs at temperatures above the onset of Fe magnetic (SDW) order and the orthorhombic structure could continue to exist in the superconducting phase too. Similar arguments can be used for the current phase diagram of $\text{EuFe}_2(\text{As}_{1-x}\text{P}_x)_2$ where most likely AF (Eu) and SC phase coexist with the orthorhombic phase. Detailed analysis of the tetragonal to orthorhombic distortion on the stability of the FM and AF Eu^{2+} sublattice on our samples is in progress. In general, a FM phase is not favorable for SC within s-wave pairing mechanisms, because the Zeeman effect arising due to ferromagnetism will strongly disfavor the singlet formation, which will eventually lead to the breakdown of the Cooper pairs. FM ordering of Eu^{2+} ions will result in an internal magnetic field of reasonable strength due to its large spin value $S=7/2$, which is detrimental to the SC occurring in the FeAs layers. Hence we believe that the previous reports^{21,24} on the coexistence of SC and Eu-FM in $\text{EuFe}_2(\text{As}_{0.73}\text{P}_{0.27})_2$ and $\text{EuFe}_2(\text{As}_{0.7}\text{P}_{0.3})_2$ might probably be related to inhomogeneous phosphorus doping concentration in polycrystalline samples.³⁴ In general, single crystals are compositionally more homogeneous than polycrystalline samples, and the presence of even a few percent volume fraction of the superconducting phase in a given sample, should result in a strong drop (not zero) in the resistivity measurements. In our single crystals, with $x=0.26$ and 0.38 , we did not observe any such drop in resistivity. At this juncture, we would also like to note that, by crushing a single crystal of $\text{EuFe}_2(\text{As}_{0.62}\text{P}_{0.38})_2$ into a powder we repeated all our measurements and did not notice any change in our descriptions (*i.e.* only FM ordering of the Eu^{2+} moments was observed, but no SC phase transition).

For a microscopic understanding of the inter-layer coupling of the Eu^{2+} moments in $\text{EuFe}_2(\text{As}_{1-x}\text{P}_x)_2$, we have carried out total energy calculations using the full-potential local orbital code (FPLO).³⁵ We used the Perdew-Wang³⁶ flavor of the exchange-correlation potential and the energies were converged on a dense k -mesh consisting of 20^3 points. The localized Eu 4f states were treated on a mean-field level by using the LSDA+U

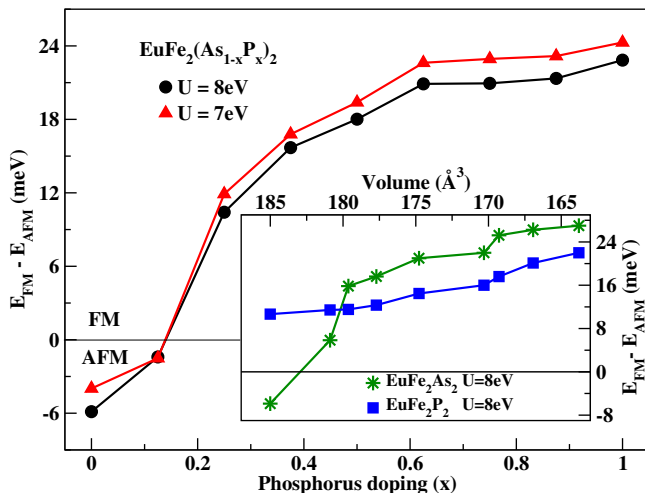


FIG. 5. (Color online) Energy difference between FM and AF aligned Eu^{2+} moments along the c -axis, as a function of Phosphorus content in $\text{EuFe}_2(\text{As}_{1-x}\text{P}_x)_2$. Along the y -axis, the ground state is AFM below zero and FM above zero. Inset: Energy difference (same as main panel) as a function of reduced volume for the two end-members EuFe_2As_2 and EuFe_2P_2 . The data points in the inset and the main panel have a one-to-one correspondence.

(local-spin-density-approximation + strong correlations) approach, applying the so called “atomic limit” (AL) double-counting scheme.³⁷ In general, the physically relevant value of the strong Coulomb repulsion U_{4f} of the Eu^{2+} ion are inferred from various spectroscopy techniques, especially by photoemission spectroscopy (PES) experiments. Owing to the lack of such experiments for EuFe_2As_2 , we have therefore used a U_{4f} value of 7-8 eV.³⁸ The robustness of our results and consequently the interpretations were checked for consistency with varying U_{4f} values. The Fe $3d$ states were treated on an itinerant level (LSDA) without additional correlations. The partial P substitution was modeled by the construction of supercells of various sizes. The randomness in possible substitution positions were taken into account by allowing phosphorus to occupy different possible combinations of the four-fold $4e$ As sites. The lattice parameters for the various supercells were obtained by interpolating linearly the experimental data reported in Table I. The As/P z -position was kept fixed at $z=0.362$ throughout. Based on density functional theory calculations, we have previously¹⁹ shown that the Eu and Fe sublattices are quite de-coupled in EuFe_2As_2 . This result is also corroborated experimentally by showing that the Eu^{2+} moments only play a minor role in the electronic transport properties.³⁹ Presently, our goal is to obtain an estimate for the Eu inter-layer coupling below T_N or T_C , while the Fe sublattice is retained in the SDW pattern. The results from our calculations are collected in Fig. 5. For $x < 0.2$, the ground state of $\text{EuFe}_2(\text{As}_{1-x}\text{P}_x)_2$ is A-type AF, consistent with the above mentioned experimental results. The energy difference between the AF (ground

state) and FM alignment of the Eu^{2+} moments is quite small (0 to 6 meV per formula unit). This implies a rather weak inter-layer coupling for the Eu sublattice. Any small external effects (impurities, doping, external pressure and fields) can easily flip the Eu spins from AF to FM. This has also been shown experimentally by Xiao and co-workers⁴⁰ for the parent compound EuFe_2As_2 , wherein below T_N they observe a field-induced spin reorientations to the FM state for an applied field of just 1 T in the ab -plane and at 2 T along the c -axis. For $x > 0.2$, FM inter-layer coupling between the Eu^{2+} moments becomes favorable (*i.e.* ground state is FM) and continues to remain so for larger P substitutions, consistent with the present experimental observations. The Fe sublattice remains magnetic for $0 \leq x \leq 0.875$ with a slight reduction of the individual magnetic moments with increasing phosphorus content. The Fe sublattice becomes non-magnetic for the end member of this substitution series EuFe_2P_2 , while the rare-earth Eu remains divalent in the entire substitution range. These results are also consistent with the recently reported experimental findings of Feng and co-workers²³ for EuFe_2P_2 . Another recent report by Sun and collaborators⁴¹ witness a valence change of europium from a $2+$ to a $3+$ state in $\text{EuFe}_2\text{As}_{1.4}\text{P}_{0.6}$ at ambient conditions along with a SC transition at 19.4 K. They also suggest that the FeAs layers receive the additional charges arising from this valence transition, which in turn steers the onset of SC. This valence change behavior seems rather counterintuitive, since the end member EuFe_2P_2 is a well known ferromagnet with divalent europium.⁴² One should also note that other alkaline-earth based members of the ‘122’ family have been shown to superconduct upon isovalent doping either on the Fe site or the As site, without the possibility of additional charges entering the FeAs layers.^{14,15,26-28} LDA+ U calculations favor integer occupation, but a qualitative description of the valence transitions can be obtained from such calculations.⁴³ Therefore, we investigated the possibility of such a valence change ($\text{Eu}^{2+} \rightarrow \text{Eu}^{3+}$) in our calculations and found that europium always favors the divalent state in the entire substitution range.

As mentioned earlier, without the introduction of additional holes or electrons, isovalent doping of As by P introduces “chemical pressure” in $\text{EuFe}_2(\text{As}_{1-x}\text{P}_x)_2$. Phosphorus ion is smaller than the arsenic ion, and the lattice parameters shrink rather anisotropically (c/a decreases significantly) with increasing phosphorus content (compare Table I) and the lattice becomes more 3-dimensional. Similar anisotropic changes to the lattice parameters along with a strong decrease of the c/a ratio leading to bulk SC was also observed for isovalent substitution of Fe by larger Ru atoms.¹⁵ The substitution of As by P and as well as the decrease in the volume of the unit cell together influence the magnetism of the Eu sublattice. In order to de-couple these two effects; substitution and volume reduction and henceforth obtain a deeper understanding of the chemistry and lattice effects respectively, we performed two further calculations:

(i) parent compound EuFe_2As_2 as a function of reduced volume; and (ii) end member EuFe_2P_2 as a function of reduced volume. The previously described supercell calculations provide information on the effects of substitution, while the current calculations explain the effects of the lattice. Our findings are summarized in the inset of Fig. 5. The data points in the inset have a one-to-one correspondence with the doping (x) values in the main panel. The ground state of EuFe_2As_2 changes from AF to FM earlier than that of $\text{EuFe}_2(\text{As}_{1-x}\text{P}_x)_2$. The As $4p$ states are more extended than P $3p$ states, which when combined with a strong decrease of the c -axis tends to influence the inter-layer magnetic interaction of the Eu^{2+} ions more than phosphorus. On the contrary, Eu^{2+} moments in EuFe_2P_2 remain FM for all volumes in our calculations. The reported ambient conditions volume from experiments for EuFe_2P_2 is 163.79 \AA^3 (Ref. 23) with FM aligned Eu ions. Expanding this lattice to 185 \AA^3 (room-temperature volume of EuFe_2As_2) reduces the strength of the FM interaction between the inter-layer Eu ions, but does not flip the spins. Combining these results, we infer that the lattice effects play the major role in influencing the interplay of Eu-magnetism in $\text{EuFe}_2(\text{As}_{1-x}\text{P}_x)_2$.

In summary, we have systematically grown high quality single crystals and studied the transport, mag-

netic and thermodynamic properties on a series of $\text{EuFe}_2(\text{As}_{1-x}\text{P}_x)_2$ samples and explore the details of the interplay of AF and FM phase of Eu^{2+} moments with the SC phase as a function of phosphorus doping. We find that the SDW transition associated with the Fe moments can be suppressed upon P doping and obtain a bulk SC phase transition up to 28 K for $x=0.2$. Further increasing the P content, SC vanishes and Eu^{2+} ordering changes from AF to FM. Our results suggest that SC and FM phases compete with each other. Careful analysis also shows that the bulk SC phase co-exists with Eu AF phase, possibly in orthorhombic symmetry. Density functional theory based calculations also witnesses a change in the ordering of the Eu^{2+} moments from AF to FM with increasing phosphorus content. Further analysis allows us to infer that the lattice effects is more conducive to the AF to FM transformation of the Eu^{2+} moments, rather than the phosphorus substitution itself. More microscopic experiments like μSR , low temperature powder diffraction, NMR etc. are currently in progress to confirm the different phases reported here.

The authors would like to thank, C. Geibel, Y. Tokiwa and K. Winzer for discussion and help. We acknowledge financial support by the DFG Research Unit SPP-1458.

-
- ¹ N. D. Mathur, F. M. Grosche, S. R. Julian, I. R. Walker, D. M. Freye, R. K. W. Haselwimmer, G. G. Lonzarich, *Nature* **394**, 39-43 (1998).
 - ² O. Stockert, E. Faulhaber, G. Zwirgagl, N. Stüßer, H.S. Jeevan, M. Deppe, R. Borth, R. Kuchler, M. Loewenhaupt, C. Geibel, and F. Steglich, *Phys. Rev. Lett.* **92**, 136401 (2004).
 - ³ N. K. Sato, N. Aso, K. Miyake, R. Shiina, P. Thalmeier, G. Varelogiannis, C. Geibel, F. Steglich, P. Fulde, and T. Komatsubara, *Nature* **410**, 340 (2001).
 - ⁴ Y. Kamihara, T. Watanabe, M. Hirano, and H. Hosono, *J. Am. Chem. Soc.* **130**, 3296 (2008).
 - ⁵ H. Takahashi, K. Igawa, K. Arii, Y. Kamihara, M. Hirano, and H. Hosono, *Nature*, **453**, 376 (2008).
 - ⁶ X. H. Chen, T. Wu, G. Wu, R. H. Liu, H. Chen and D. F. Fang, *Nature*, **453**, 761 (2008).
 - ⁷ G.F. Chen, Z. Li, D. Wu, G. Li, W.Z. Hu, J. Dong, P. Zheng, J.L. Luo, and N.L. Wang, *Phys. Rev. Lett.* **100**, 247002 (2008).
 - ⁸ M. Rotter, M. Tegel, and D. Johrendt, *Phys. Rev. Lett.* **101**, 107006 (2008).
 - ⁹ H. S. Jeevan, Z. Hossain, D. Kasinathan, H. Rosner, C. Geibel, and P. Gegenwart, *Phys. Rev. B* **78**, 092406 (2008).
 - ¹⁰ K. Sasmal, B. Lv, B. Lorenz, A. M. Guloy, F. Chen, Y. Y. Xue, and C. W. Chu, *Phys. Rev. Lett.* **101**, 107007 (2008).
 - ¹¹ G. Wu, H. Chen, T. Wu, Y. L. Xie, Y. J. Yan, R. H. Liu, X. F. Wang, J. J. Ying, and X. H. Chen, *J. Phys.: Condens. Matter* **20**, 422201 (2008).
 - ¹² F. C. Hsu, J. Y. Luo, K. W. Yeh, T. K. Chen, T. W. Huang, Phillip. M. Wu, Y. C. Lee, Y. L. Huang, Y. Y. Chu, D. C. Yan, and M. K. Wu, *Proc. Natl. Acad. Sci. USA* **105**, 14262(2008).
 - ¹³ A. Leithe-Jasper, W. Schnelle, C. Geibel, and H. Rosner, *Phys. Rev. Lett.* **101**, 207004 (2008).
 - ¹⁴ D. Kasinathan, A. Ormeci, K. Koch, U. Burkhardt, W. Schnelle, A. Leithe-Jasper, and H. Rosner, *New J. Phys.* **11**, 025023 (2009).
 - ¹⁵ W. Schnelle, A. Leithe-Jasper, R. Gumeniuk, U. Burkhardt, D. Kasinathan, and H. Rosner, *Phys. Rev. B* **79**, 214516 (2009).
 - ¹⁶ C. Wang, S. Jiang, Q. Tao, Z. Ren, Y. Li, L. Li, C. Feng, J. Dai, G. Cao, and Zhu'an Xu, *Euro. Phys. Lett.* **86**, 47002 (2009).
 - ¹⁷ S. Jiang, H. Xing, G. Xuan, C. Wang, Z. Ren, C. Feng, J. Dai, Zhu'an Xu, and G. Cao, *J. Phys.: Condens. Matter* **21**, 382203 (2009).
 - ¹⁸ C. F. Miclea, M. Nicklas, H. S. Jeevan, D. Kasinathan, Z. Hossain, H. Rosner, P. Gegenwart, C. Geibel, and F. Steglich, *Phys. Rev. B* **79**, 212509 (2009).
 - ¹⁹ H. S. Jeevan, Z. Hossain, Deepa Kasinathan, H. Rosner, C. Geibel, and P. Gegenwart, *Phys. Rev. B* **78**, 052502 (2008).
 - ²⁰ Y. Qi, Z. Gao, L. Wang, D. Wang, X. Zhang, and Y. Ma, *New J. Phys.* **10**, 123003 (2008).
 - ²¹ Z. Ren, Q. Tao, S. Jiang, C. Feng, C. Wang, J. Dai, G. Cao, and Z. Xu, *Phys. Rev. Lett.* **102**, 137002 (2009).
 - ²² T. Terashima, M. Kimata, H. Satsukawa, A. Harada, K. Hazama, S. Uji, H. S. Suzuki, T. Matsumoto, and K. Murata, *J. Phys. Soc. Jpn.* **78**, 083701 (2009).
 - ²³ C. Feng, Z. Ren, S. Xu, Z. Xu, G. Cao, I. Nowik, I. Felner, K. Matsubayashi, and Y. Uwatoko, *Phys. Rev. B* **82**, 094426 (2010).
 - ²⁴ A. Ahmed, M. Itou, S. Xu, Zhu'an Xu, G. Cao, Y. Sakurai, J. Penner-Hahn, and A. Deb, *Phys. Rev. Lett.* **105**, 207003 (2010).

- (2010).
- ²⁵ Z. Ren, X. Lin, Q. Tao, S. Jiang, Z. Zhu, C. Wang, G. Cao, and Z. Xu, *Phys. Rev. B* **79**, 094426 (2009).
 - ²⁶ S. R. Saha, N. P. Butch, K. Kirshenbaum, and Johnpierre Paglione, *Phys. Rev. B* **79**, 224519 (2009)
 - ²⁷ L. J. Li, Y. K. Luo, Q. B. Wang, H. Chen, Z. Ren, Q. Tao, Y. K. Li, X. Lin, M. He, Z. W. Zhu, G. H. Cao, and Z. A. Xu, *New J. Phys.* **11**, 025008 (2009)
 - ²⁸ N. Kumar, S. Chi, Y. Chen, K. G. Rana, A. K. Nigam, A. Tamizhavel, W. Ratcliff II, S. K. Dhar, and J. W. Lynn, *Phys. Rev. B* **80**, 144524 (2009)
 - ²⁹ S. Thirupathaiah, E.D.L. Rienks, H.S. Jeevan, R. Ovsyanikov, E. Slooten, J. Kaas, E. van Heumen, S. de Jong, H.A. Duerr, K. Siemensmeyer, R. Follath, P. Gegenwart, M.S. Golden, J. Fink, arXiv:1007.5205
 - ³⁰ L. Rettig, R. Corts, S. Thirupathaiah, P. Gegenwart, H.S. Jeevan, T. Wolf, U. Bovensiepen, M. Wolf, H.A. Drr, J. Fink, arXiv:1008.1561
 - ³¹ D. Wu, G. Chanda, H. S. Jeevan, P. Gegenwart, M. Dressel, arXiv:1011.1207
 - ³² S. Jiang, H. Xing, G. Xuan, C. Wang, Z. Ren, C. Feng, J. Dai, Z. Xu, G. Cao, *J. Phys.: Condens. Matter*, **21**, 382203 (2009)
 - ³³ S. Nandi, M. G. Kim, A. Kreyssig, R. M. Fernandes, D. K. Pratt, A. Thaler, N. Ni, S. L. Budko, P. C. Canfield, J. Schmalian, R. J. McQueeney, and A. I. Goldman, *Phys. Rev. Lett.* **104**, 057006 (2010).
 - ³⁴ Note that in Ref. 24, despite the coexistence of SC and Eu-FM order, a competition of SC and Fe-FM was claimed.
 - ³⁵ K. Koepernik, and H. Eschrig, *Phys. Rev. B* **59**, 1743 (1999).
 - ³⁶ J. P. Perdew and Y. Wang, *Phys. Rev. B* **45**, 13244 (1992).
 - ³⁷ M. T. Czyżyk and G. A. Sawatzky, *Phys. Rev. B* **49**, 14211 (1994).
 - ³⁸ Another way of obtaining an estimate for ‘U’ is the energy difference of the spectral weight transfer due to a valence change of Eu from a 2+ to a 3+ state. A recent report (Ref. 41) evidences such a valence transition under pressure for EuFe₂As₂ and consistent with our assumptions for ‘U_{4f}’, the energy difference between the main Eu²⁺ peak and the satellite Eu³⁺ peak is ≈ 8 eV.
 - ³⁹ T. Terashima, N. Kurita, A. Kikkawa, H. S. Suzuki, T. Matsumoto, K. Murata, and S. Uji, *J. Phys. Soc. Japan* **79**, 103706 (2010)
 - ⁴⁰ Y. Xiao, Y. Su, W. Schmidt, K. Schmalzl, C. M. N. Kumar, S. Price, T. Chatterji, R. Mittal, L. J. Chang, S. Nandi, S. K. Dhar, A. Tamizhavel, and T. Brueckel, *Phys. Rev. B* **81**, 220406 (2010).
 - ⁴¹ L. Sun, J. Guo, G. Chen, X. Chen, X. Dong, W. Lu, C. Zhang, Z. Jiang, Y. Zhou, S. Zhang, Y. Huang, Q. Wu, X. Dai, Y. Li, J. Liu, and Z. Zhao, *Phys. Rev. B* **82**, 134509 (2010).
 - ⁴² E. Mörsen, B. D. Mosel, W. Müller Warmuth, M. Reehuis, and W. Jeitschko, *J. Phys. Chem. Solids* **49**, 785 (1988).
 - ⁴³ R. Gumeniuk, M. Schmitt, C. Loison, W. Carrillo-Cabrera, U. Burkhardt, G. Auffermann, M. Schmidt, W. Schnelle, C. Geibel, A. Leithe-Jasper, and H. Rosner, *Phys. Rev. B*, in press (2010).